Journal of Physics and Chemistry of Solids 75 (2014) 379–383

Contents lists available at ScienceDirect

Journal of Physics and Chemistry of Solids

journal homepage: www.elsevier.com/locate/jpcs

Stability and electronic properties of carbon in α-Al_2O_3

Jiajie Zhu [a,c], K.P. Muthe [b], Ravindra Pandey [a,*]

[a] Department of Physics, Michigan Technological University, Houghton, MI 49931, USA
[b] Bhabha Atomic Research Center, Mumbai, India
[c] Department of Physics, Tongji University, Shanghai 200092, PR China

ARTICLE INFO

Article history:
Received 2 July 2013
Received in revised form
8 November 2013
Accepted 12 November 2013
Available online 19 November 2013

Keywords:
A: Oxides
A: Optical materials
C: Ab initio calculations
D: Defects
D: Electronic structure

ABSTRACT

The stability and electronic properties of carbon in α-Al_2O_3 are investigated using density functional theory. In the host lattice, the substitutional C prefers the Al site under the O-rich conditions, whereas the O site is preferred by carbon under the Al-rich conditions. The calculated results predict a direct relationship between the thermodynamic and optical transition levels with the degree of the local distortion induced by C in the alumina lattice. We also find C at the O site acts as a charge compensator to stabilize the F^+ center, thereby enhancing the TL signal at 465 K. Also, C at Al site can serve as electron traps for TL emission process in α-Al_2O_3.

1. Introduction

Aluminum oxide (Al_2O_3) was one of the earliest oxide materials considered as a phosphor material for thermoluminescence (TL) based radiation measurements in spite of its low sensitivity [1]. The desirable properties of Al_2O_3 including the high thermo-chemical stability continued to attract scientific efforts which aspired to improve sensitivity of the material [2]. Considering that the exoelectron emission, and thereby the luminescent properties of oxides can be improved by creating deficiency of oxygen in the lattice [3,4], Akselrod and his colleagues synthesized a new phosphor Al_2O_3:C in a strongly reducing ambience of graphite whose TL sensitivity was significantly higher than the standard LiF:Mg, Ti [5]. The oxygen-deficient phosphor, Al_2O_3:C has a wide dynamic range for radiation measurements extending from μGy to Gy. Significantly, this phosphor besides the customary thermal stimulation also permits dose measurements through the use of light [6]. As a result, Al_2O_3:C has found applications in various branches of optically stimulated luminescence (OSL) based dosimetry, e.g. personnel, neutron, space, medical, environmental, and emergency dosimetry [7].

Although Al_2O_3:C is being used and investigated extensively, the role of carbon in rendering this phosphor remarkably sensitive towards radiation is not well understood [8]. It has a characteristic TL peak in the temperature range of 450–480 K. The emission spectra of this peak consists of 420 nm emission which has been attributed to radiative decay of the F centers (i.e. oxygen vacancies that have captured two electrons) and another emission observed at 320 nm to that of the F^+ centers (i.e. oxygen vacancy with one captured electron) [5]. We note that the reducing environment of carbon present during the crystallization of alumina from melt induces a large number of oxygen vacancies which lead to the creation of F and F^+ centers serving as recombination centers in the lattice. Since the formation of F^+ centers requires presence of charge compensators in the lattice, this explanation relies on the premise that Al^{3+} is substituted by C^{2+} in the lattice [9]. On the other hand, the mismatch in the ionic radii of Al^{3+} and C^{2+} together with the fact C in the reducing ambience is known to substitute oxygen in TiO_2 [10,11] have given an alternative scenario in which C^{4-} substitutes the oxygen, and may have only a marginal existence at the interstitial sites for the higher doping levels [8]. Either of these proposals assumes the role of carbon to be that of a dopant implying its direct involvement in improving the dosimetric sensitivity of Al_2O_3 via chemical modifications in the lattice.

Interestingly though, a comparable improvement in the TL properties has also been observed even when the Al_2O_3 samples were annealed in the presence of molybdenum [12]. It was also noticed that the concentration of defects appreciably increased along the direction of crystal growth from alumina melt. This has led to a viewpoint that the extreme sensitivity of alumina is basically of intrinsic nature arising due to presence of the associative centers comprising of an oxygen vacancy and an aluminum ion displaced to a new geometric position in the lattice. Rather than that of dopants, the role of agents like C and Mo is

* Corresponding author. Tel: +1 9064872086.
E-mail address: pandey@mtu.edu (R. Pandey).

0022-3697/$ - see front matter © 2013 Elsevier Ltd. All rights reserved.
http://dx.doi.org/10.1016/j.jpcs.2013.11.005

restricted to the mere production of effects which involve the weakening of the bonds in the host lattice and the formation of the oxygen vacancies leading to the case where alumina can be regarded as un-doped [13].

It is well known that for a phosphor to be sensitive towards radiation, it must possess a large concentration of traps, besides the recombination centers in the lattice. In this regard, the positron annihilation spectroscopic experiments carried out on a single crystal of Al_2O_3 that were annealed in the presence of graphite have indicated ingress of carbon into aluminum vacancies. Thus, the results have provided direct evidence that association of carbon with aluminum vacancies leads to creation of the effective dosimetric traps facilitating improved dosimetry sensitivity of the material [2].

This multifarious nature of the influence of C on the Al_2O_3 and its topicality prompted us to undertake a detailed investigation of stability and electronic properties of C in Al_2O_3 using first-principle methods based on density functional theory. We are not aware of any theoretical studies investigating stability and electronic properties of C in α-Al_2O_3, though the defect electronic levels of C in γ-Al_2O_3 were previously investigated using the quasi-particle calculations within the G_0W_0 approximation [14].

2. Theoretical method

The electronic structure calculations were performed using the projector augmented plane-wave (PAW) method as implemented in Vienna ab initio simulation package (VASP) [15,16]. The generalized gradient approximation (GGA) of Perdew, Burke and Ernzerhof (PBE) was used for the exchange-correlation potential [17]. The total energy of the system is well converged using the plane-wave cutoff energy of 520 eV [18]. The Brillouin zone integrations were performed with the $8\times8\times8$ k-point mesh. The structural parameters of the supercell and the internal coordinated of all atoms in the supercell are relaxed until the force on each atom is less than 0.01 eV/Å.

Incorporation of C in α-Al_2O_3 is simulated by the $(2\times2\times2)$ supercell which consists of 80 atoms. Generally, the error in the supercell calculations is introduced by the unphysical interaction between the defect and its periodic images. For the $(2\times2\times2)$ supercell, the distance between the defect and its mirror image is about 10.2 Å. A comparison of the results obtained from $(2\times2\times2)$ and $(3\times3\times3)$ supercell calculations suggest the difference of the order of 0.2 eV in the defect formation energy, though the electronic structure remains nearly the same. We refer the difference to be 'error' in the defect formation energy. Note that the distance between the defect and its mirror image is about 15.3 Å in the $(3\times3\times3)$ supercell.

In our calculations, the total number of electrons in the unit cell is summation over all atoms for the neutral defect in the lattice. For positive or negative charge state of the defect, an electron is removed from or added to the unit cell. The presence of a uniform background charge is assumed to compensate the charged defects in the lattice. Note that Al, O and C atoms are associated with the $3s^23p^1$, $2s^22p^4$and $2s^22p^2$ valence electrons, respectively in our calculations.

The formation energy $\Delta H^f(D,q)$ of a defect in the charge state q depends on both the Fermi level and chemical potentials of species related to the defect and can be given as [19]

$$\Delta H^f(D,q)=\Delta E(D,q)+\sum_i n_i\mu_i+q(E_F+E_{VBM}) \quad (1)$$

$\Delta E(D,q)$ is the difference between the total energy of the supercell containing a point-defect D in the charge state q and that of the supercell representing the perfect lattice. n_i and μ_i are the number of atoms removed from the supercell and chemical potentials of the constituent, *i.* E_{VBM} and E_F are the valence-band maximum (VBM) and Fermi level, respectively. E_F then ranges from VBM to the conduction-band minimum (CBM) of the lattice. We take the values of E_F from 0 to the band gap value of 8.7 eV of α-Al_2O_3 [18].

The defect transition energy level $\varepsilon(q/q')$ is defined as the Fermi level where the formation energy of defect D in charge state q is equal to charge state q', i.e.

$$\varepsilon(q/q')=[\Delta H^f(D,q,E_F=0)-\Delta H^f(D,q',E_F=0)]/(q-q') \quad (2)$$

Since other related byproduct cannot be precipitated, the chemical potentials of Al, O and C in α-Al_2O_3 are restricted by following conditions

$$3\mu_O+2\mu_{AL}=E(Al_2O_3) \quad (3)$$

$$\mu_C=E(C) \quad (4)$$

$$\mu_O\le E(O) \quad (5)$$

$$\mu_{AL}\le E(Al) \quad (6)$$

$$\mu_O+\mu_C\le E(CO) \quad (7)$$

$$2\mu_O+\mu_C\le E(CO_2) \quad (8)$$

$$3\mu_C+4\mu_{AL}\le E(Al_4C_3) \quad (9)$$

where $E(Al_2O_3)$ is the total energy of the bulk α-Al_2O_3 and $E(O)$ is half of the total energy of O_2.

3. Results and discussion

Fig. 1(a) and (b) shows a fragment of the perfect α-Al_2O_3, which has a rhombohedral structure. Note that α-Al_2O_3 has the crystal symmetry of R-3c (No. 167). The calculated structural parameters at the GGA-DFT level of theory are in excellent agreement with the experimental values [20]. For example, the lattice constant is 5.18 Å and the corresponding experimental value is 5.136 Å. The angle between a and b axes is 55.29° as compared to the experimental value of 55.28°.

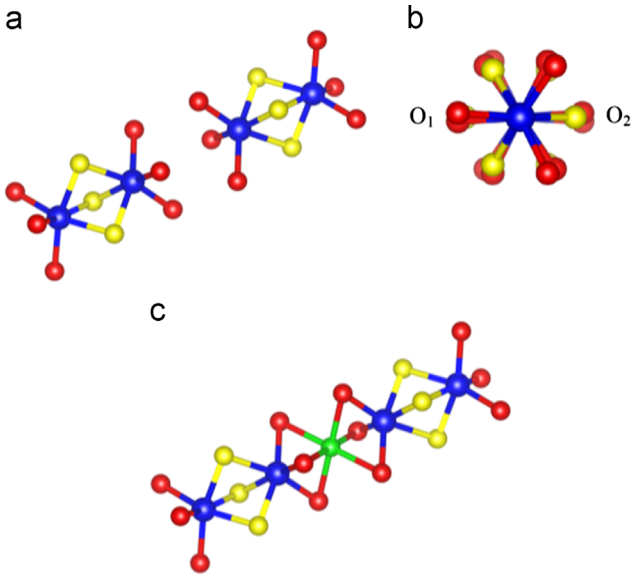

Fig. 1. A schematic diagram of α-Al_2O_3. (a) Side view and (b) top view; (c) C at the interstitial site. [Al: blue, O_1: red, O_2: yellow and C: green.] (For interpretation of the references to color in this figure legend, the reader is referred to the web version of this article.)

The coordination number of Al and O atom in the lattice are six and four, respectively. The Al atom is surrounded by three nearest-neighboring O atoms (O_I) and three next-nearest-neighboring O atoms (O_{II}) with the distances of 1.87 Å and 1.99 Å, respectively. For an O atom, there are two nearest-neighboring Al atoms (Al_I) and two next-nearest-neighboring Al atoms (Al_{II}). The calculated Al–O bond distances are similar to the ones calculated previously using the extended tight-binding method [21].

Incorporation of C in α-Al_2O_3 can be done at either the interstitial (C_i) or the substitutional Al (C_{Al}) and O (C_O) sites. At the interstitial site, C is surrounded by two Al atoms and six O_1 atoms yielding its coordination number to be eight in the lattice (Fig. 1(c)). Table 1 lists the structural properties of the optimized configurations of C doped α-Al_2O_3 including the local distortions induced by carbon in the oxide lattice.

Since α-Al_2O_3 is mainly an ionic material, magnitude of the local distortion is mainly determined by the defect charge state of C in the lattice. Additionally, a large difference between the atomic radius of the dopant C (0.91 Å) and the host lattice atoms, Al (1.82 Å), and O (0.73 Å) may also play an important role in inducing the local distortions in the lattice. For C substituting O (i.e. C_O), the neighboring Al atoms relax outward, and the magnitude of distortion becomes large as the defect charge state changes from −1 to +1. On the other hand, the neighboring O atoms response to C substituting Al (i.e. C_{Al}) in different ways; the O_I atoms move inwardly whereas the O_{II} atoms move outwardly. Such type of lattice distortion can be attributed to the covalent nature of the C–O_I bond in the lattice. For the interstitial C atom, a relatively large displacement of the neighboring oxygens as compared to that of the neighboring Al atoms in the lattice is predicted (Fig. 2, Table 1).

Table 1
Carbon in α-Al_2O_3: the lattice distortion with respect to the perfect α-Al_2O_3 for which R_{Al-O_1} = 1.87 Å, R_{Al-O_2} = 1.99 Å, $R_{interstitial-Al}$ = 1.99 Å, and $R_{interstitial-O}$ = 2.00 Å.

Charge state	Substitutional-C_O (Å)		Substitutional-C_{Al} (Å)		Interstitial-C_i (Å)	
	ΔR_{C-Al_I}	$\Delta R_{C-Al_{II}}$	ΔR_{C-O_I}	$\Delta R_{C-O_{II}}$	ΔR_{C-Al}	ΔR_{C-O_I}
−1	+0.03	−0.01	−0.22	+0.5	−0.05	+0.26
0	+0.08	+0.11	−0.46	+0.67	−0.01	+0.17
+1	+0.17	+0.17	−0.56	+0.78	+0.09	+0.09

We now calculate the dopant formation energy which can provide the guidance about its solubility in the host lattice. It is well known that low formation energy of a dopant indicates the possibility of incorporating the dopant in the lattice, and vice versa. Furthermore, the dopant formation energy is directly related to its atomic chemical potentials which can be adjusted by changing the partial pressure or concentration of the element during the growth or annealing condition.

The calculated dopant formation energy using Eq. (1) for both O-rich and Al-rich conditions are shown in Fig. 3. Note that the formation energy of a dopant of a given charge state is a function of the Fermi energy. We find that C_{Al} and C_O have the lowest formation energies over the whole range of Fermi level for O-rich and Al-rich conditions, respectively, thus suggesting that C can be incorporated at Al or O site in α-Al_2O_3. However, this is not the case for the interstitial C which has relative high formation energy in the lattice. In α-Al_2O_3 crystal grown by temperature gradient technique (TGT), carbon is suggested to replace oxygen and only a small volume of carbon may occupy interstitial site, which is in good agreement with our calculated results [8]. The PAW-GGA calculations on C doped MgO also find the Mg-rich environment to be preferred for the incorporation of C in the oxide lattice [22]. Note that −1 charge state of C_O in the Al-rich conditions can serve as a charge compensator for the F^+ center in the lattice that is related to the TL peak at around 465 K [8]. On the other hand, C_{Al} in −1 charge state can act as a charge compensator for the F^+ center in the O-rich condition.

The thermodynamic transition levels associated with C in α-Al_2O_3 are illustrated in Fig. 4. These levels can be detected by the deep level transient spectroscopy (DLTS), where the final

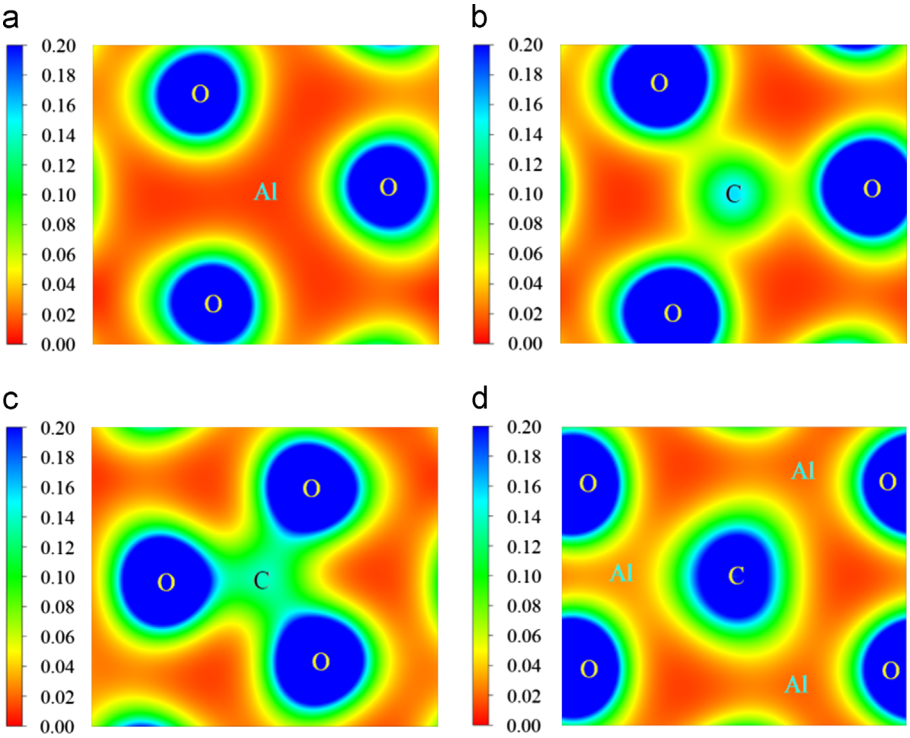

Fig. 2. Charge density contours projected at the (111) plane of (a) perfect α-Al_2O_3, (b) α-Al_2O_3:C_i, (c) α-Al_2O_3:C_{Al}, and (d) Al_2O_3:C_O.

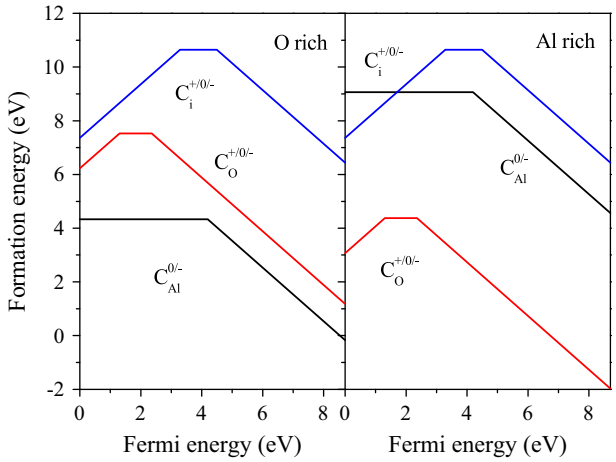

Fig. 3. The calculated formation energies of C_{Al}, C_O and C_i as a function of Fermi energy (E_F) under (a) O-rich, and (b) Al-rich conditions. Zero of E_F is taken to be the top of the valence band. The superscript and slope of the segment represent the dopant charge state in the lattice.

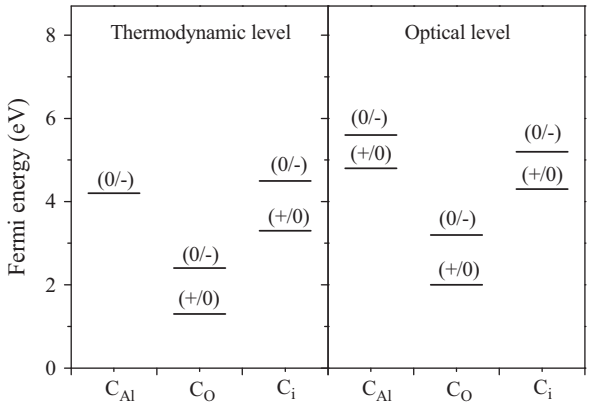

Fig. 4. The calculated thermodynamic and optical transition levels for C_{Al}, C_O and C_i. Zero of Fermi energy is taken to be the top of the valence band.

charge state completely relaxes to its equilibrium configuration after transition. The calculated results show that C_{Al} introduces a thermodynamic transition level $\varepsilon(0/-)$ at 4.2 eV above the top of the valence band. As shown in Fig. 3, C_{Al} is stable in its neutral charge state for $E_F < 4.2$ eV and its -1 charge state is energetically preferred for $E_F > 4.2$ eV. On the other hand, C at the O site induces two thermodynamic transition levels ranging from 0.9 to 2.4 eV. For C_i, the levels range from 3.1 to 4.5 eV. Overall, the results predict that incorporation of C is electrical inactive in α-Al_2O_3 since its levels are not close to either the valance band maximum (VBM) or the conduction band minimum (CBM).

Fig. 4 also shows the optical transition levels associated with C in α-Al_2O_3. An optical transition level can be probed by emission and absorption spectroscopy [23], and can be calculated using the same atomic configuration for the initial and final charge states of the dopant in the lattice. It is the same as the thermodynamic transition level if the electronic transition is not phonon-assisted transition in the lattice. The calculated results find a significantly large shift associated with C_{Al}-$\varepsilon(0/-)$ transition in α-Al_2O_3. The calculated shift between the optical and thermodynamic transition levels is related to the difference between the corresponding lattice distortions in the ground state configurations. This is indeed the case as shown in Table 1 where the lattice distortion in the ground state of C_{Al}^0 is larger than that in the ground state of C_{Al}^- in α-Al_2O_3.

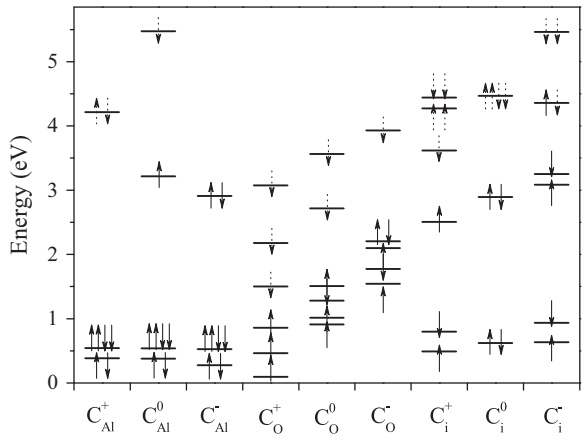

Fig. 5. The single-particle dopant levels associated with C_{Al}, C_O and C_i in α-Al_2O_3. Zero is taken to be top of the valence band. The superscripts represent the dopant charge states. The solid and dot arrows correspond to occupied and unoccupied states, respectively.

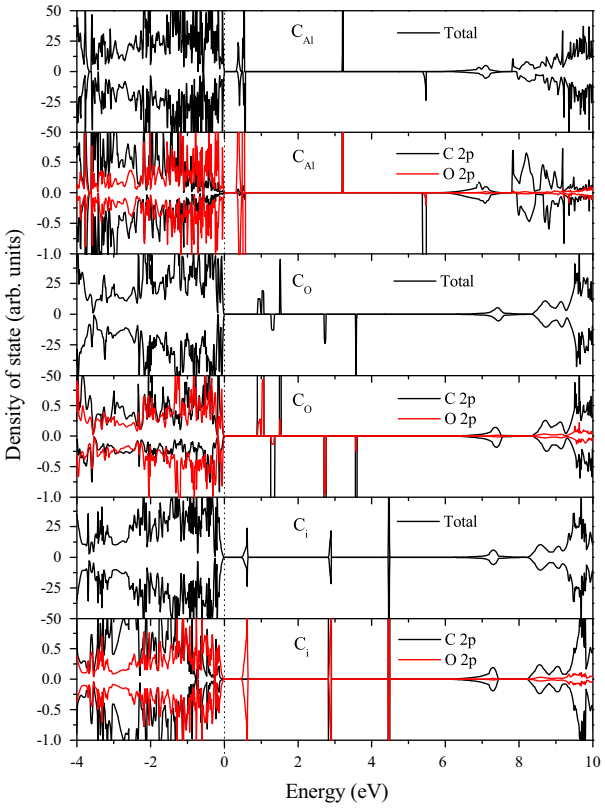

Fig. 6. Total and atomic projected density of states of neutral C_{Al}, C_O and C_i. Zero of the energy is aligned to the valance band maximum (VBM).

The calculated single-particle levels associated with C_{Al}, C_O and C_i are shown in Fig. 5. The substitutional C at the Al site induces shallow acceptor-like levels near VBM. On the other hand, the substitutional C at the O site appears to be associated with deep acceptor-like levels within the band gap. No donor-like levels are induced by carbon since the highest partially occupied level induced by C_i^- is at 1.5 eV below the conduction band minimum CBM in α-Al_2O_3. Our results are similar to the calculated results of carbon in γ-Al_2O_3 [14]. The difference in location and occupation of dopant level may be attributed to the different crystal structures since α-Al_2O_3 is rhombohedral and γ-Al_2O_3 is cubic.

In order to get further insights into electronic properties of C doped α-Al_2O_3, we have calculated the total and atomic projected density of states (DOS). The total DOS of the oxide doped with carbon shows appearance of the gap states within the gap which is calculated to be about 6.0 eV at the GGA-DFT level of theory (Fig. 6). The uppermost valence band of α-Al_2O_3 is mainly composed of the O-2p states, whereas the gap states consisted of mainly with O-2p states with a small degree of mixing with C-2p states. Relative to VBM, the gap states are located at about ~0.45, 3.2, and ~5.3 eV for C_{Al}, ~0.98, ~1.4, 2.7 and 3.6 eV for C_O, and 0.6, 2.9 and 4.5 eV for C_i in the oxide lattice. Additionally, an unoccupied state close to CBM for the case of C_{Al} may contribute to the TL emission as an electron trap since the trap depth calculated from the TL glow curve is about ~0.72 eV below CBM in the oxide lattice [6].

4. Summary

The calculated results based on density functional theory predict the dominance of C_{Al} for the O-rich conditions and that of C_O for the Al-rich conditions in α-Al_2O_3. The calculated results therefore affirm the suggestion of incorporation of carbon at the oxygen sites in the oxide lattice under the reducing conditions by experiments [8]. The calculated lattice distortions induced by C at the Al site are relatively large which are reflected in the predicted difference between thermodynamic and optical transition levels of C_{Al}-$\varepsilon(0/-)$. C at the O site is not likely to distort the lattice significantly, and can act as a charge compensator to stabilize the F^+ center thereby enhancing the TL signal at 465 K. Furthermore, C at Al site induces some unoccupied states near CBM that can serve as electron traps for TL emission process in α-Al_2O_3.

Acknowledgment

Jiajie Zhu acknowledges the financial support from Department of Physics, Michigan Technological University during his visit.

References

[1] J.K. Rieke, F. Daniels, J. Phys. Chem. 61 (1957) 629.
[2] K.P Muthe, K. Sudarshan, P.K. Pujari, M.S. Kulkarni, N.S. Rawat, B.C. Bhatt, S.K. Gupta, J. Phys. D: Appl. Phys. 42 (2009) 105405.
[3] V.S. Kortov, Jpn. J. Appl. Phys. 24 (Sup. 24-4) (1985) 65.
[4] V.S. Kortov, Jpn. J. Appl. Phys. 24 (Sup. 24-4) (1985) 69.
[5] M.S. Akselrod, V.S. Kortov, D.J. Kravetsky, V.I. Gotlib, Radiat. Prot. Dosim. 32 (1990) 15.
[6] B.G. Markey, L.E. Colyott, S.W.S. McKeever, Radiat. Meas. 24 (1995) 457.
[7] E.G. Yukihara, S.W.S. McKeever, Optically Stimulated Luminescence: Fundamentals and Applications, John Wiley & Sons, New York, 2011.
[8] X. Yang, H. Li, Q. Bi, Y. Cheng, Q. Tang, J. Xu, J. Appl. Phys. 104 (2008) 123112.
[9] M.S. Akselrod, V.S. Kortov, D.J. Kravetsky, V.I. Gotlib, Radiat. Prot. Dosim. 33 (1990) 119.
[10] S.U.M. Khan, M.A. Shahry, W.B. Ingler Jr., Science 297 (2002) 2243.
[11] T. Ohno, T. Tsubota, K. Nishijima, Z. Miyamoto, Chem. Lett. 33 (2004) 750.
[12] J. Kvapil, Z. Vitmvas, B. Perner, J. Kvapil, B. Manek, O. Adametz, J. Kubelka, Krist. Technol. 15 (1980) 859.
[13] T.I. Gimadova, T.S. Bessonova, I.A. Tale, L.A. Avvakumova, S.V. Bodyachevsky, Radiat. Prot. Dosim. 33 (1990) 47.
[14] K. Sankaran, G. Pourtois, R. Degraeve, M.B. Zahid, G.M. Rignanese, J. Van Houdt, Appl. Phys. Lett. 97 (2010) 212906.
[15] G. Kresse, J. Furthmuller, Phys. Rev. B 54 (1996) 11169.
[16] G. Kresse, D. Joubert, Phys. Rev. B 59 (1999) 1758.
[17] J.P. Perdew, K. Burke, M. Ernzerhof, Phys. Rev. Lett. 77 (1996) 3865.
[18] K Matsunaga, T. Tanaka, T. Yamamoto, Y. Ikuhara, Phys. Rev. B 68 (2003) 85110.
[19] A. Soon, X. Cui, B. Delley, S. Wei, C. Stampfl, Phys. Rev. 79 (2009) 35205.
[20] H. d'Amour, D. Schiferl, W. Denner, H. Schulz, W.B. Holzapfer, J. Appl. Phys. 49 (1978) 4411.
[21] I.P. Batra, J. Phys. C: Solid State Phys. 15 (1982) 5399.
[22] Y. Zhang, H. Liu, J. Wu, X. Zuo, IEEE Trans. Magn. 47 (2011) 2928.
[23] C.G. Van de Walle, J. Neugebauer, J. Appl. Phys. 95 (2004) 3851.